



**DOI:** https://doi.org/10.58233/hj1U5s75

# Novel ATR-FTIR and UV-Vis spectral markers for assessing the Prooxidant/Antioxidant Balance (PAB) in white wines

Stylianos Neonakis<sup>1</sup>, Stella A. Ordoudi<sup>1</sup>

<sup>1</sup> Laboratory of Oenology and Alcoholic Beverages, Department of Food Science and Technology, School of Agriculture, Aristotle University of Thessaloniki, 57001, Thermi, Thessaloniki, Greece

Abstract. The browning index (BI), based on the absorbance at 420 nm, is a common oxidation marker in white wines, typically measured after thermal stress (50-60 °C for 5 up to 12 days) in air-saturated wines. However, oxidative shifts begin much earlier, with initiation and propagation reactions altering the prooxidant/antioxidant balance (PAB) before browning appears. This study investigates whether non-targeted fingerprinting by ATR-FTIR and UV-Vis spectroscopy can capture early-stage compositional changes that occur during the first hours of the treatment (1 - 8 hours at 60 °C). Moschofilero wines (2023 vintage, two bottling batches) were used for this purpose. Spectral data were analyzed using Principal Component Analysis (PCA) and Generalized Two-Dimensional Correlation Spectroscopy (2D-COS). Key oenological and antioxidant-related parameters (free and total SO<sub>2</sub>, pH, redox potential, total phenols, DPPH•, FRAP) were also monitored. Time-related patterns of UV-Vis absorbance at 350–370 nm, possibly linked to Fe(III)-tartrate complexes and ATR-FTIR shifts at 3000–3600 cm<sup>-1</sup>, due to hydrogen bond rearrangements, were observed. They coincided with a rise in redox potential (+106 to +123 mV) and free SO<sub>2</sub> depletion (below 30 mg/L), indicating a progressive decline of wine redox buffering capacity. In contrast, the total phenolic content and antioxidant activity remained unchanged. Validation with additional samples (Asirtiko, Malagouzia, vintages 2022, 2023) confirmed the potential of the identified markers. These findings highlight a novel approach for interpreting UV-Vis and ATR-FTIR spectroscopic data to monitor early oxidation in white wines. Further validation is ongoing to support the development of rapid, nondestructive, and data-driven tools for proactive wine stability management and more sustainable oenological practices.

# 1. Introduction

Susceptibility to oxidation is a major concern for winemakers, who must make key decisions throughout the production process based on either direct or indirect risk assessment. In the case of white wines, the risk of browning during storage is typically evaluated under accelerated thermal stress conditions. A standardized method, originally developed five decades ago by Singleton and Kramling [1], laid the foundation for several modifications and is still widely used today. The original assay involves incubating air-saturated test samples (pretreated with bentonite) and nitrogen-flushed control samples at 55 °C for five days in the dark. More recent protocols eliminated the use of bentonite and nitrogen pretreatment, extending the incubation period up to 12 days [2, 3]. The oxidation risk, referred to as the Browning Index (BI), is assessed by measuring absorbance at 420

nm, a single wavelength in the visible region. For white wines, this value may increase significantly over the monitoring period. Thus, oxidative susceptibility is evaluated based on the level of browning at the chosen endpoint. However, this endpoint is selected arbitrarily, and a standardized threshold for BI interpretation does not yet exist. Only a few studies have adopted a kinetic approach to monitor the evolution of browning markers [2, 4].

Browning is difficult to attribute to specific compounds; one proposed pathway involves the formation of yellow-orange adducts of glyoxylic acid and catechin, particularly in the presence of metal ions, which leads to the generation of reactive quinones and subsequent polymerization reactions. While increasing temperature or pH can accelerate browning, it is the interplay of various redoxactive species within the wine matrix that ultimately drives the progression of oxidation [3, 4]. Some years ago,

Sioumis et al. [2] reported that the browning is accompanied by a reduction in the wine ferric-reducing capacity, suggesting a decline in antioxidant potential. However, as their results also imply, early oxidation events before visible browning may involve more complex redox dynamics, which are not fully captured by endpoint measurements. So far, these early events have not been explored for diagnostic purposes. It can be suggested though that, during the early stages, the wine maintains a pro-oxidant/antioxidant balance (PAB) until a critical shift that favors oxidation-promoting species [5].

Alternative accelerated browning tests employ thermal incubation after chemical oxidation by hydrogen peroxide or acetaldehyde and enzymatic oxidation by laccase or electrochemical oxidation in a specialized instrument [6-8]. Because the focus was on the assessment of BI, none of the relevant studies exploited whole UV-Vis spectra instead of a single wavelength. Recently, Miao and Waterhouse [9] introduced a novel parameter, the "potential wine shelf-life", based on the observation that most white wines begin to show oxidation-related changes when free SO<sub>2</sub> falls below 10 mg/L. Rather than relying on A<sub>420</sub> readings, the authors proposed a quantitative shelf-life model after monitoring the molar ratio of SO<sub>2</sub>:O<sub>2</sub> consumption over a five-day incubation at 45 °C.

Most of the tests described above require several days to reach a steady-state endpoint and may involve chemical reagents, increasing both cost and environmental impact. In the search for rapid, greener, and smart quality control tools in winemaking, non-destructive spectroscopic techniques are gaining growing interest. Over the past two decades, the use of visible and mid-infrared spectroscopy has shown great potential for quantitative analysis and diagnostic applications in wines [10, 11]. However, it remains unclear whether the whole UV-Vis and mid-infrared spectra of white wines can capture meaningful information about early oxidation events.

Building on this evidence, our study aims to explore whether non-destructive spectroscopic methods (UV-Vis and ATR-FTIR) can detect early-stage shifts in the prooxidant/antioxidant balance (PAB), beyond the contribution of phenolic antioxidants alone. Samples from a monovarietal white wine were incubated over eight hours at 60 °C. Spectral data were analyzed using Principal Component Analysis (PCA) to uncover time-related patterns and potential diagnostic markers. In addition, Generalized Two-Dimensional Correlation Spectroscopy (2D-COS) was used to evaluate the sequence and progression of molecular interactions during the first hours of the treatment [12]. To complement the spectroscopic data, we monitored changes in electrochemical parameters (pH, redox potential, free and total SO<sub>2</sub>), as well as classical antioxidant capacity indices, including Total Phenol Content, DPPH radical scavenging activity, and Ferric Reducing Antioxidant Power (FRAP).

#### 2. Materials and Methods

# 2.1. Wine samples

Monovarietal white wine (Moschofilero, Peloponnese, Greece) from a single vintage (2023) and two different production lots was purchased from the local market and stored at 20 ± 2 °C until treatment. Once opened, the wines were homogenized and subjected to treatments in three replicates. Samples of different monovarietal dry white wines (Asirtiko, Malagousia, n = 4) that comprised a validation test set were obtained by Oenopolis laboratory (Drama, Greece) that performs regular quality controls and certifications. Aliquots of around 50 mL were transferred to our laboratory and kept at -20 °C. All samples were centrifuged (4 °C, 1968 g, 10 min) before treatments and analyses.

#### 2.2. Accelerated oxidation test

The model used to assess wine oxidation was a modification of that described by Singleton and Kramling (1976) for browning development [1]. Fifty mL of centrifuged wine were placed in a 500 mL closed flask. To achieve oxygen saturation, the wine sample was vigorously shaken for 10 seconds, followed by uncapping the flask for 5 seconds to allow air exchange. This process was repeated three times. Each sample (50 mL) was placed in a 65 mL screw-cap glass vial (9.2 cm in length and 3.5 cm internal diameter), with the headspace above the wine being at 23% of the vial volume. Samples were exposed to a constant temperature of  $60 \pm 0.5$  °C in an Orbit Environ-Shaker 3527 oven (Lab-line Instruments, USA), in the dark to prevent light exposure. Replicate vials were collected every hour over 8 hours and placed in a water bath until the sample temperature remained at  $21.5 \pm 0.5$ °C.

#### 2.3. Electrochemical tests

#### 2.3.1. Redox potential and pH

Measurements of the Oxidation-Reduction Potential (ORP) and pH were carried out by the multiparameter modular system HI6000 (HANNA instruments, Italy). All measurements were performed at room temperature.

#### 2.3.2. Free and Total SO<sub>2</sub> content

Sulfur dioxide (its free and total form) was determined according to a modified Ripper method using the automatic titration device Iodolyser (Laboratoires Dujardin Salleron, France), according to the instructions of the manufacturer. Free SO<sub>2</sub> was calculated by mixing 25 mL of wine with diluted H<sub>2</sub>SO<sub>4</sub> solution (1+3, v/v). Total SO<sub>2</sub> quantification was performed by mixing 10 mL of wine with 2 mL of 2N NaOH, allowing it to stand for 5 min, followed by the addition of 20 mL of diluted H<sub>2</sub>SO<sub>4</sub> (1+10, v/v). Titration was performed with automatic stirring.

#### 2.4. Antioxidant capacity assessment

### 2.4.1. Total phenol content (TPC)

A modified Folin-Ciocalteau method, adapted from OIV-MA-AS2-10 [13] was used to assess the total phenol content (TPC). In brief, 100  $\mu L$  of sample and 500  $\mu L$  of Folin-Ciocalteau reagent were mixed in a 10 mL volumetric flask. After 3 min, 1.5 mL of saturated (20 %, w/v) sodium carbonate solution was added to the reaction mixture. The solution was diluted with water to 10 mL and the absorbance at 750 nm was measured after 1 h against a blank solution. Gallic acid was used as an external standard and the results were expressed as mg/L gallic acid equivalents (mg GAE/L). All determinations were performed in duplicate at room temperature.

# 2.4.2. DPPH\* scavenging activity

The DPPH• assay was adapted from Ordoudi et al. [14]. Briefly,  $100~\mu L$  of undiluted wine were mixed with 2.9~mL of a 0.1~mM methanolic solution of DPPH• and the mixture was stored in the dark at room temperature. After 30~minutes, the absorbance was measured at 515~nm. Trolox was used as an external standard, and results were expressed as mM Trolox equivalents (mM TE).

# 2.4.3. Ferric reducing antioxidant power assay (FRAP)

The total reducing capacity of wine samples was determined according to Benzie and Strain [15]. 2.85 mL of working FRAP reagent was incubated at 37  $^{\circ}\text{C}$  for four minutes and then 150  $\mu\text{L}$  of diluted sample were added. The mixture was stored for 30 minutes at room temperature and the absorbance was read at 593 nm. Trolox was used to obtain a standard curve and the results were expressed as mM Trolox equivalents (mM TE).

### 2.5. Spectroscopic examination

#### 2.5.1. UV-Vis spectroscopy

The UV-Vis spectra were recorded in the region 200-700 nm using a UV-Vis GENESYS 50 Spectrophotometer (Thermo Fisher Scientific, USA) and a 10 mm path length quartz cuvette. Each wine sample was measured against distilled water as a blank. Percentages of changes in  $A_{420}$  values (%  $\Delta A_{420}$ ) were calculated over the incubation period, as a browning index [4].

### 2.5.2. ATR-FTIR spectroscopy

ATR-FTIR spectra were acquired using a 6700 IR (Jasco, Essex, UK) spectrometer equipped with a DLaTGS detector, a high-throughput Single Reflection ATR with diamond crystal, and complemented by the Spectra Manager software (Jasco, Essex, UK). 64 scans per sample (400  $\mu$ L) were accumulated in the absorbance mode and recorded at 4 cm<sup>-1</sup> resolution, covering a range from 4000

to 650 cm<sup>-1</sup>. The spectrum was collected against air as background and corrected by the CO<sub>2</sub>, H<sub>2</sub>O and ATR correction options of the software. After each measurement, the crystal was rinsed with isopropanol and dried. Three spectra per sample were collected and the data were further processed as follows; smoothing with the Savitzky-Golay algorithm (second-degree polynomial, 15 points), exclusion of the data among 1800–2600 and 3600–4000 cm<sup>-1</sup>, normalization with the Standard Normal Variate function (SNV) or sample-wise baseline correction with the aid of SIMCA© 18.0 software (Umetrics, Umeå, Sweden).

#### 2.6. Statistical analysis

#### 2.6.1. Multivariate data analysis

Multivariate analysis was conducted on raw and preprocessed UV-Visible and ATR-FTIR spectral data of wine samples. The data were mean-centered and analyzed using the Principal Component Analysis (PCA) algorithm in the SIMCA© 18.0 software (Umetrics, Umeå, Sweden). The score [t] and variable loading [p] plots for Principal Components that explained > 95% of the total data variance were monitored for similarity/difference patterns and identification of potentially diagnostic spectral features (absolute p loading >0.05) [16].

# 2.6.2. Generalized Two-Dimensional Correlation Spectroscopy (2D-COS)

Generalized Two-Dimensional Correlation Spectroscopy (2D-COS) was performed by 2D Shige software [17], according to the theory of 2D-COS analysis [12]. Incubation time (1, 2, 4, 8 h) was the perturbation variable of the dynamic spectra that resulted in the generation of 2D-COS synchronous and asynchronous maps. The autopeaks of the former map (always positive) are located on the central diagonal and represent spectral changes (e.g. within a region) that take place simultaneously (correlated in-phase) over two or more independent spectra (crosspeaks) located off the central diagonal. Cross-peaks of a given colour, representing a positive sign, indicate that the intensity of the corresponding bands or regions is increasing or decreasing simultaneously. Cross-peaks of different colours representing a negative sign, indicate a reversal trend. Asynchronous maps capture out-of-phase correlated changes. Their signs (marked with two different colours) may provide useful information about the sequence of events over the incubation time [12]. In our study, red colour showed that  $x_1$  spectral (horizontial axis) changes occur before their correlated alterations in y<sub>1</sub> spectra (vertical axis), while blue colour showed the opposite sequence  $(x_1 \text{ after } y_1)$ .

#### 3. Results and Discussion

#### 3.1. Basic markers of oxidative status

All the control and test samples exhibited very low  $A_{420}$ , between 0.05 to 0.08 a.u., close to the spectral baseline. The Browning Index (BI) increased by almost 34 %, although no visual differences were perceived over the eight-hour incubation period (Figure 1).



Figure 1. Wine samples before and after incubation at 60 °C for four and eight hours.

The pH values remained stable during this treatment, ranging from 3.28 (control) to 3.31 - 3.33. ORP fluctuated from +105.7 to +122.7 mV, suggesting the ongoing consumption of reducing agents. Indeed, while total SO<sub>2</sub> content gradually fell from 160.0 to 90 mg/L the free SO<sub>2</sub> levels were rapidly consumed and reached 30 mg/L (p < 0.05) after four hours of incubation. Thus, out of the electrochemical indices employed in this study, only the SO<sub>2</sub> content measurements might be useful for early oxidation in line with assessments, previous observations [9].

The total phenol content of the white wine sample also remained unchanged during the short incubation period (around 270 to 284 mg GAE/L). A similar trend was observed for the DPPH radical scavenging activity (0.59 to 0.60 mM TE) that is mainly ascribed to phenolic moieties, but also for the Ferric-Reducing Antioxidant Power (1.70 to 1.73 mM TE), which refers to reducing species. These results imply that any changes in the composition of the matrix during the first eight hours of incubation are not explained by phenolic reactivity indices.

#### 3.2. UV-Vis spectral data analysis

UV-Vis spectra of 18 wine samples (2 control and 8×2 test samples) were averaged and cropped to exclude the region 450–600 nm that was devoid of signals. The overlapped spectra are shown in Figure 2a.

Principal Component Analysis of the remaining data yielded two principal components (PCs) that explained 99.5% of the total variance. The samples were scattered over both sides of the PC1 axis ( $R^2 = 88.8\%$ ) which probably captures ongoing molecular interactions over the short incubation period. Of note, the [t1] score values for both lots of bottled wine tended to increase up to around seven to eight hours. (Figure 2b). Greater variance occurred during the first four to five hours, after which the samples were all clustered in a group with t1 > 0. Based on the highest loadings of the two PCs (data not shown), the

most important spectral variables represented the slope of the downcurve among 350–372 nm. These subtle changes in the fine structure of the spectrum were revealed as most responsible for the time-related pattern of scores during the first eight hours. This pattern followed a log-linear relationship ( $R^2 = 0.706$ ), suggesting an exponential evolution of the system over this early period (Figure 2c).

The diagnostic importance of the region was also evidenced on the synchronous map of the dynamic UV-Vis spectra by one autopeak at 350–360 nm (Figure 3a). A close inspection of the asynchronous map (Figure 3b) allowed us to suggest that absorbance shifts in the 368-440 nm region were likely to chronologically precede.

The increasing absorbance in the UV-Vis region among 320 to 380 nm could originate from invisible to yellow pigments that are rapidly formed as intermediate products during the thermal oxidation period. This region is highly unspecific; apart from flavonol moieties like quercetin and rutin, other absorbing species involve Fe(III)-tartrate and/or reduced glutathione complexes that may accumulate during the early oxidation stages, especially when there is no light protection [18]. Thus, the gradual widening of the UV-Vis spectral curve could be due to charge transfer and the formation of those species.

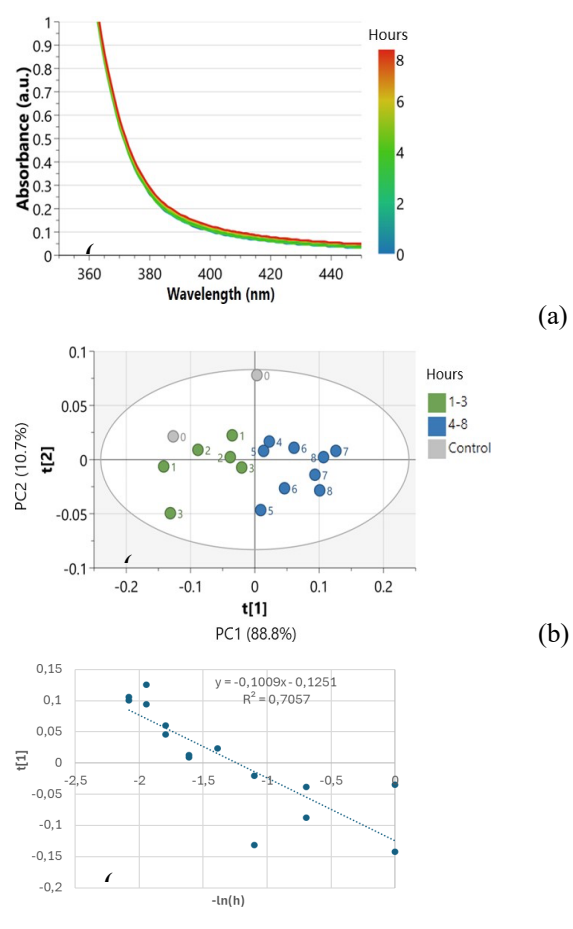


Figure 2. UV-Visible spectra (a), PCA score scatter plot (b), and semi-log linear decay of t[1] over the incubation time (c) of wine samples before (control) and during treatment (1-8) h). Each dot in the scatter plot t[1]/t[2] represents the average spectrum of a different batch of bottled wine and is coloured to highlight the stage of heating (green – 1-3 h, blue – 4-8 h).

(c)

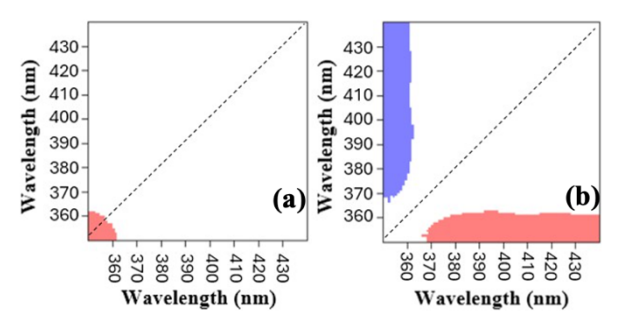


Figure 3. Generalized 2D-Correlated UV-Vis spectral data over the region 350-450 nm . (a) Synchronous map with autopeaks on the central diagonal (red colour). Cross peaks of the same colour represents simultaneous increase or decrease. (b) Asynchronous map where, the red colour indicates that  $x_1$  spectra (horizontial axis) changes occur before the  $y_1$  spectra (vertical axis) alteration, while blue colour shows the opposite. For more details, please refer to the section 2.6.2.

# 3.3. ATR-FTIR spectra

The ATR-FTIR spectra of the samples under study are shown in Figure 4. The spectra were visually identical to each other while their fingerprint region (650-1800 cm<sup>-1</sup>) was typical of a hydro-alcoholic mixture. Thus, apart from the broad band at around 1600–1650 cm<sup>-1</sup> due to the abundance of water, ethanol and/or other primary alcohols can also be recognized by characteristic methyl/methylene deformation and C-O stretching vibrational bands at around 1042, 1085, but also at 872 cm<sup>-1</sup>. Many other weaker bands in the region among 1100 and 1550 cm<sup>-1</sup> contribute to the wine spectral fingerprint at a given time. For example, C-H bending vibrations from structural moieties of phenols typically absorb between 1400 and 1500 cm<sup>-1</sup> [11, 19].

On the other hand, complex hydrogen-bond networks among wine constituents, with fundamental vibrations at >3100 cm<sup>-1</sup> overlap the methyl- stretching bands at around 1980 cm<sup>-1</sup> [19]. This is probably the reason why the whole region above 2600 cm<sup>-1</sup> is usually neglected in relevant wine studies as non-useful for quantitative FTIR models [11]. In our study, multivariate analysis was applied to the entire ATR-FTIR spectrum, excluding only the CO<sub>2</sub>related band (2300-2400 cm<sup>-1</sup>) and other signal-devoid regions (see 2.5.2). An exploratory approach was followed to fine-tune the parameters and obtain parsimonious PCA models. As an example, only two Principal Components (PCs) were found to explain 98.7 % of total variance (PC1=94.3% and PC2=4.37%) in the full-spectrum, preprocessed data. However, by analysing only the fingerprint region, four PCs were required to explain 98.4% of the total variance (PC1=57.3%, PC2=35.6%, PC3=4.6%, PC4=0.9%). This finding prompted us to further explore the modeled spaces and identify possible relevance to the evolution of oxidation. Figure 5a shows the corresponding scatter plot of raw, uprocessed data over the first two PCs that explained 97.2% of the total variance. Based on this plot, the wines that were incubated at 60 °C over eight hours were found to scatter across the second PC in a timerelated pattern. A gradual increase in t[2] values was due to greater variance in the bands at 1620-1640 and 670 cm<sup>-1</sup>. This observation could be related with the

ongoing molecular interactions with water molecules, including possibly aromatic moieties.

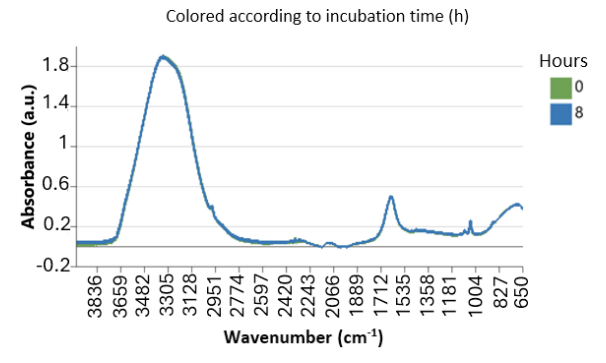
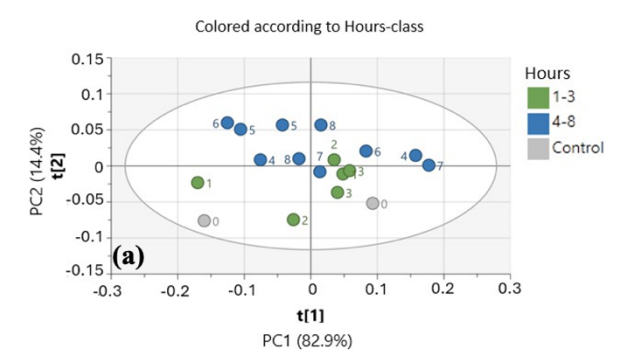
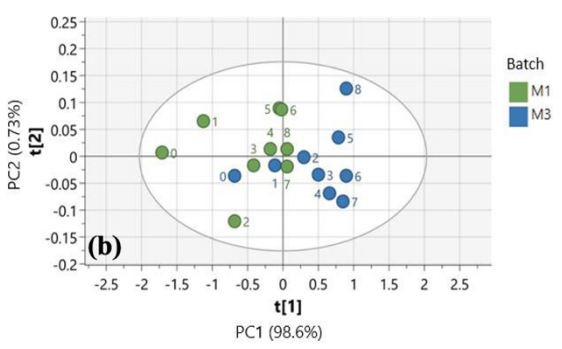


Figure 4. ATR-FTIR spectra of wine samples before (0) and after 8 hours of incubation at  $60~^{\circ}\text{C}$ .

Interestingly, the analysis of the region between 2700 and 3600 cm<sup>-1</sup> alone (Figure 5b), helped to capture a great amount of variance across a single component (PC1=98.6%). Figure 5b highlights that the two different wine batches evolved with distinct t[1] patterns over the first four to five hours after which they remained unchanged until the endpoint.





**Figure 5.** PCA score scatterplots of ATR-FTIR spectral data of control and test wine samples. The t[1]/t[2] scores are calculated from (a) raw, unprocessed data over the region 650-1800 cm<sup>-1</sup>, (b) smoothed, normalized data over the region 2700-3600 cm<sup>-1</sup>. Each dot represents the average spectrum of a different batch of bottled wine and is coloured to highlight the stage of heating (green -1-3 h, blue -4-8 h).

Synchronous mapping through 2D-COS (Figure 6a) revealed only one autopeak across 3090 to 3256 cm<sup>-1</sup> that is indicative of shifts in the prooxidant/antioxidant balance. Based on asynchronous mapping (Figure 6b), this is the result of a cascade of early initiation reactions that caused primarily changes in the -O--H absorption (3411–3588 cm<sup>-1</sup>), then, in methyl group stretching (2902–2936 and 2968–2980 cm<sup>-1</sup>).

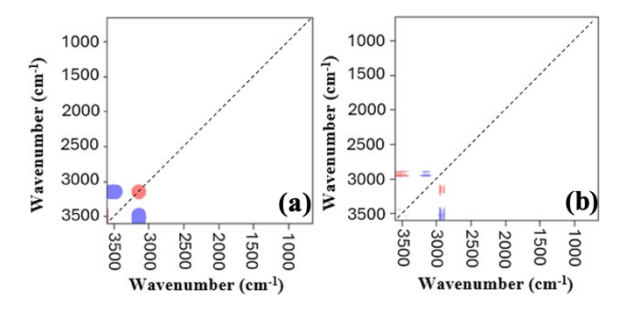
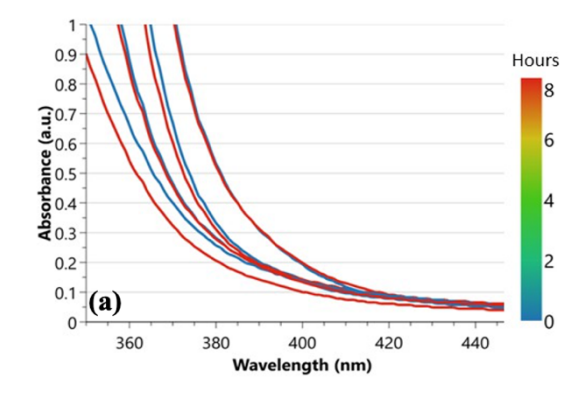


**Figure 6.** Synchronous (a) and asynchronous (b) maps of 2D-Correlated ATR-FTIR spectral data over the regions 650-3600 cm<sup>-1</sup>. For more details, please refer to the section 2.6.2.

#### 3.4. Validation tests

For validation purposes, the UV-Vis and ATR-FTIR spectroscopic features of white wines that were exposed in our study as PAB markers were also sought in a set of four additional wine samples. According to the information provided by Oenopolis laboratory (Drama, Greece), the were dry, monovarietal (Asirtiko: A1-2; Malagouzia: MA1-2), from two vintages (2023: A2, MA1-2; 2022: A1), different vine locations but also wineries across Northern Greece (Drama, Serres, Chalkidiki). The same thermal treatment conditions were applied, that is, all wine samples were incubated at 60 °C for a total of eight hours. The spectral data that were acquired before and after treatment were used for further multivariate analysis. Of note, the A<sub>420</sub> values of the wines before treatment were close to the baseline (about 0.1 a.u). However, the shape of the spectra in the region 350-450 nm varied a lot (Figure 7a); most importantly, the slope of the downcurve was already much lower, compared with those presented in Figure 2a. The BI values remained low (between 4 to 13% increase) and no colour alteration was perceived at the endpoint of incubation. As a result of the great variance in the shape of curves, their t[1] scores could not be explained by the UV-Vis-based pattern discussed earlier (data not shown).

On the other hand, the validation set samples were found to be more homogeneously distributed in the ATR-FTIR modeled spaces. Figure 7b illustrates the pattern of their t[1]/t[2] score values, as explained by the model of raw, fingerprint data (see Figure 5a for comparison). In that case, only the sample no 7 was found to be an outlier across t[1]. The t[2] values of thermally treated wines varied across both sides of the PC2 axis. We explored whether the source of this variation could be related with the PAB status by measuring the redox potential of the wines after incubation. Of note, the latter values were found to range from +157 to +208 mV, in a similar trend to that of the t[2] values.



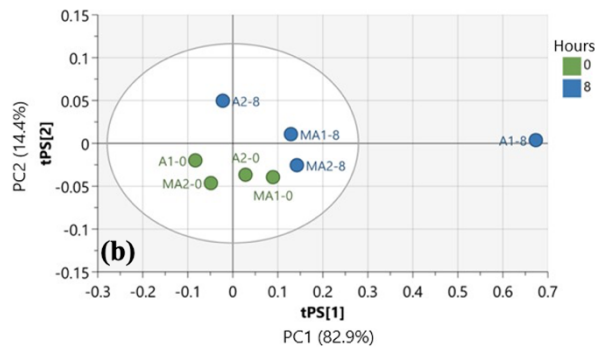


**Figure 7.** (a) UV-Visible spectra and (b) predicted PCA scatter plot of the validation set samples (A1, A2, MA1, MA2) before (0 h) and after (8 h) incubation at 60 °C.

These findings could be interpreted in terms of PAB status considering also the accompanying metadata and other reference test results. For example, the outlier in the ATR-FTIR model corresponded to A1, a sample from 2022 vintage that evolved with a distinct pattern, especially in the region 1630-1640 cm<sup>-1</sup>. The wine A2, presenting the highest t[2] score value among the validation set samples, was the one with the highest redox potential after the 8- hour incubation. Another interesting result referred to MA2, the richest in TPC (around 467 to 475 mg GAE/L) that presented the lowest t[2] value among the validation samples. In this round of analyses it was verified that the fingerpint ATR-FTIR region of the treated wines captures diagnostic information about their susceptibility to oxidation. It is important to stress that, our non-targeted fingerprinting approach might offer such type of information rapidly, within a working day.

# 4. Conclusion

Our results offer preliminary evidence that UV-Vis and ATR-FTIR spectroscopic examination can capture early molecular events related to oxidation in white wines. Through multivariate data analysis and two-dimensional correlation spectroscopy, subtle spectral changes were identified, particularly in the 350–370 nm (UV-Vis) and >3100 cm<sup>-1</sup> (ATR-FTIR), which showed time-related variance, aligned with free SO<sub>2</sub> depletion and shifts in the prooxidant/antioxidant balance.

This study is in progress. Further validation across storage conditions but also different wine types and vintages is needed to confirm the diagnostic potential of the novel markers. Overall, these findings may contribute

to the development of rapid, non-destructive tools to assess oxidation susceptibility and support more data-driven and sustainable practices in wine stability management.

#### 5. Acknowledgements

The authors would like to thank the Oenopolis Laboratory (Drama, Greece) for providing wine samples and useful metadata for validation tests.

#### References

- 1. V.L. Singleton, T.E. Kramling, Am. J. Enol. Vitic. 27, 157-160 (1976).
- 2. N. Sioumis, S. Kallithraka, D.P. Makris, P. Kefalas, Food Chem. 94, 98–104 (2006).
- 3. L. Ma, A.L. Waterhouse, Anal. Chim. Acta 1039, 162–171 (2018).
- 4. E. Vlahou, S. Christofi, I.G. Roussis, S. Kallithraka, Appl. Sci. 12, 3834 (2022).
- 5. J. Nelson, R. Boulton, A. Knoesen, Fermentation 11, 9 (2025).
- M. Palma, C. García Barroso, Eur. Food Res. Technol. 214, 441–443 (2002).
- 7. F. Coppola, L. Picariello, M. Forino, L. Moio, A. Gambuti, Molecules 26, 815 (2021).
- 8. S. Deshaies, L. Garcia, F. Veran, L. Mouls, C. Saucier, F. Garcia, Antioxidants 10, 1943 (2021).
- Y. Miao, A.L. Waterhouse, Am. J. Enol. Vitic. 76, 0760008 (2025).
- R. Joshi, R. Joshi, H.Z. Amanah, M.A. Faqeerzada, P.K. Jayapal, G. Kim, I. Baek, E.S. Park, R.E. Masithoh, B.K. Cho, Korean J. Agric. Sci. 48, 299-310 (2021).
- 11. M. Basalekou, C. Pappas, P.A. Tarantilis, S. Kallithraka, Beverages 6, 30 (2020).
- 12. I. Noda, Y. Ozaki, Two-Dimensional Correlation Spectroscopy – Applications in Vibrational and Optical Spectroscopy (John Wiley & Sons, Chichester, 2004).
- 13. OIV, Compendium of International Methods of Wine and Must Analysis (International Organisation of Vine an Wine, 2009).
- 14. S.A. Ordoudi, C.D. Befani, N. Nenadis, G.G. Koliakos, M.Z. Tsimidou, J. Agric. Food Chem. 57, 3080–3086 (2009).
- I.F.F. Benzie, J.J. Strain, Anal. Biochem. 239, 70-76 (1996).
- S.A. Ordoudi, C. Ricci, G. Imparato, M. Chroni,
  A. Nucara, A. Gerardino, F.R. Bertani, Food Chem. 455, 139822 (2024).

- 17. S. Morita, 2Dshige Software, https://sites.google.com/view/shigemorita/home/2dshige (accessed 18 January 2025).
- A.C. Clark, D.A. Dias, T.A. Smith, K.P. Ghiggino, G.R. Scollary, J. Agric. Food Chem. 59, 3575– 3581 (2011).
- 19. G. Socrates, Infrared and Raman Characteristic Group Frequencies: Tables and Charts, 3rd ed. (John Wiley & Sons, Chichester, 2004).